Graphitically encapsulated cobalt nanocrystal assemblies†

Shu-Hua Liu,[ab] Haitao Gao,[c] Enyi Ye,[a] Michelle Low,[a] Suo Hon Lim,[a] Shuang-Yuan Zhang,[ab] Xiaohui Lieu,[a] Sudhiranjan Tripathy,[a] Wolfgang Tremel[c] and Ming-Yong Han*[ab]

Received 5th March 2010, Accepted 5th May 2010
First published as an Advance Article on the web 26th May 2010
DOI: 10.1039/c0cc00242a

Graphitically encapsulated cobalt nanocrystal assemblies are chemically prepared by one-pot reaction at >380 °C followed by a reversed etching process to produce porous graphitic structure for revealing their self-assembling nature.

Very recently, great efforts have been directed to preparing various well-defined carbon-coated metal nanoparticles as an alternative to widely studied silica-coated ones.[1] In addition to amorphous carbon coating on optically active noble metal nanoparticles,[2] there is also a great focus on graphitic carbon coating of magnetic transition metal nanoparticles, which not only provides surface protection of magnetic properties against oxidation but also renders the nanoparticles water soluble by chemical functionalization for biological, catalytic and patterning applications.[3] The synthesis of such core–shell nanostructures usually involves two steps: the formation of metal nanocores and the subsequent carbon coating on them in vapor, liquid or solid phases. For example, catalytically assisted chemical vapour deposition on bare magnetic metal nanoparticles and high-temperature/H_2-reduction post-treatments of organic ligand-modified magnetic metal nanoparticles have been employed to produce graphitic carbon-coated metal nanostructures.[4] At the same time, direct solid-phase preparations of graphitically encapsulated magnetic metal nanoparticles have been demonstrated as well using direct conversion of iron stearate at 900 °C,[5] flame spray pyrolysis of a metal-containing organic precursor,[6] laser irradiation of organometallics[7] and arc-discharge/microwave-induced graphitization.[8] In this paper, we report one-pot wet-chemistry synthesis of graphitically encapsulated cobalt nanostructures at a moderate temperature of >380 °C. The mild production, hermetic protection and easy manipulation/functionalization of graphitically encapsulated metal nanostructures are suitable for diverse applications.

Graphitically encapsulated cobalt nanostructures were prepared in a mixed solution of 4 mmol preformed cobalt(II) oleate and 20 mL oleic acid. A TEM image of the as-obtained magnetic particles of ~400 nm in average size is shown in Fig. 1A. An HRTEM image of one typical single particle (Fig. 1B and inset SAED) reveals a clear (101) plane of crystalline hcp cobalt with a lattice of 0.190 nm between adjacent planes. The XRD profile in Fig. 1C confirms the formation of hcp cobalt as indicated by the (100), (002) and (101) reflection peaks at 48.6°, 52.3° and 55.8°, respectively.[4c,9] The average cobalt crystal size is calculated to be ~18.7 nm based on the Scherrer equation using the three peaks. This is in accordance with what is observed in the high-magnification TEM image of one single cobalt aggregate in Fig. 1D, which consists of many small primary cobalt nanocrystals as revealed by their boundary contrast.

Interestingly, very thin shells were also seen clearly around the cobalt nanoaggregates in Fig. 1D. TEM EDX analysis shows the co-existence of carbon and cobalt elements with an atomic ratio of ~4 : 5 by using silica- rather than carbon-coated copper grids (Fig. 1E and Fig. S1†). Furthermore, with the aid of HRTEM, the very clear shell of ~5 nm in thickness was found to have crystalline graphite structure with an interplanar distance of ~0.34 nm using fast Fourier transform analysis (Fig. 2A), consistent with that between two adjacent (200) planes of graphite.[10] Raman measurement further confirmed the formation of graphitic shells around cobalt nanoaggregates with a G-band centered at 1602 cm^{-1} and a D-band centered at 1350 cm^{-1} (lower curve in Fig. 2D).[11] In addition to the use of 4 mmol cobalt(II) oleate in oleic acid,

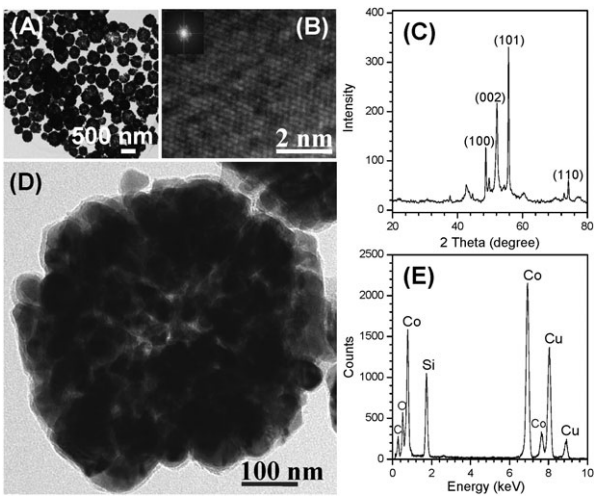

Fig. 1 (A) Low-magnification TEM image, (B) HRTEM image (inset: SAED), and (C) XRD profile of as-obtained cobalt nanostructures prepared in the presence of excess oleic acid. (D) High-magnification TEM image of one single cobalt nanostructure. (E) EDX spectrum of cobalt nanostructures.

[a] *Institute of Materials Research and Engineering, A-STAR, Singapore 117602. E-mail: my-han@imre.a-star.edu.sg; Tel: +65-68741987*
[b] *Division of Bioengineering, National University of Singapore, Singapore 117574. E-mail: biehanmy@nus.edu.sg*
[c] *Institute of Inorganic Chemistry and Analytical Chemistry, Johannes Gutenberg University, D-55128 Mainz, Germany*

† Electronic supplementary information (ESI) available: Experimental details, EDX analysis, UV-vis spectrum, TEM image, and formation scheme of graphitically encapsulated cobalt nanocrystal assemblies. See DOI: 10.1039/c0cc00242a

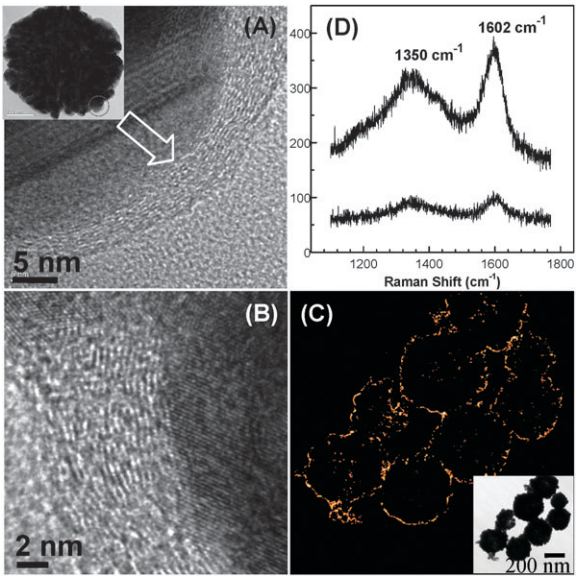

Fig. 2 (A) HRTEM image of thinner sheet-like graphitic shells on cobalt nanocores prepared in the presence of excess oleic acid. (B) HRTEM image and (C) carbon-element mapping of thicker graphitic shells on cobalt nanocores prepared in the presence of excess oleic acid together with additional sodium oleate. (D) The two Raman spectra from (A) and (B) correspond to lower and upper curves, respectively.

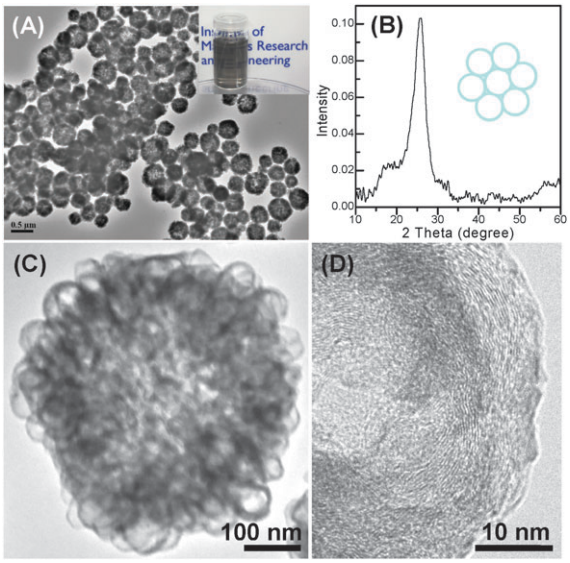

Fig. 3 (A) Low-magnification TEM image and (B) XRD pattern of graphitically encapsulated cobalt nanocrystal assemblies after strong acid etching in 2 M hydrochloric acid for 12 h. Inset in (a) shows a resulting transparent dispersion in water. (C) High magnification TEM and (D) HRTEM images of porous graphitic network from one single cobalt nanocrystal assembly after etching.

40 mmol sodium oleate was also added as a more reductive additive into the reaction system to prepare cobalt nano-aggregates. The resulting thicker graphitic shells (Fig. 2B) enabled us to directly map carbon distribution around cobalt aggregates by TEM electron energy loss spectroscopy (EELS) (Fig. 2C). Correspondingly, a stronger Raman scattering signal was observed as well in Fig. 2D (upper curve).

Although graphitic shells were clearly identified by both HRTEM and Raman spectroscopy, no characteristic XRD pattern of graphite was observed directly. One possible reason is that most of the graphitic shells around small primary cobalt nanocrystals were embedded inside their larger cobalt nanocrystal aggregates. Straightforward evidence that all the primary cobalt nanocrystals were coated with graphitic shells may come from strong acid-etching of cobalt nanocrystal aggregates. After 12-h treatment with 2 M hydrochloric acid to dissolve magnetic cobalt cores, the resulting black solution became non-magnetic with a broad absorption peak spanning 200 to 800 nm (Fig. S2†). The remaining graphitic carbon nanostructures (Fig. 3A) were clearly identified as shown in the XRD pattern (Fig. 3B). High-magnification TEM images in Fig. 3C and Fig. S3† show highly porous features with a clear contour of cobalt nanocrystal aggregates, which shows that small primary cobalt nanocrystals were coated with graphitic shells before etching (Supporting Scheme 1†). The reactive graphitic shells mediated the assembling of cobalt cores into bigger aggregates. Fig. 3D further shows the remaining graphitic shells still preserved crystalline sheet-like graphite structure after etching to remove cobalt cores.

The macroscopic assemblies of graphitically encapsulated cobalt nanocrystals exhibited room-temperature ferromagnetic properties (insert in Fig. 4A).[12] The detailed magnetic properties were studied using a SQUID magnetometer. Fig. 4A shows their M–H curves at both 5 and 300 K. The saturation magnetization (Ms) is 158 emu/g after deducting the mass of diamagnetic graphitic shells, and it is close to the Ms value of bulk cobalt (theoretical value: 162 emu/g). This result came as no surprise when we consider the good crystallinity of cobalt nanocrystals as well as the excellent graphitic shell protection of cobalt nanocrystals from natural oxidation. Meanwhile, this result also indicates ferromagnetic primary cobalt nanocrystals may be magnetically oriented during the self-assembling process mediated through the highly reactive graphitic shells. The zoomed M–H curves (Fig. 4B) show that from 5 to 300 K, the cobalt nanocrystal assemblies are ferromagnetic with a coercivity field of $\sim$850 Oe at 5 K and $\sim$550 Oe at 300 K, respectively. The absence of magnetic exchange bias showed there was no formation of a cobalt oxide layer around the cobalt cores.[13] Without the protection of graphitic shells, small cobalt nanocrystals capped with small molecular ligands are liable to oxidization, which leads to the formation of cobalt oxide shells around cobalt nanocrystals at ambient conditions or hollowed cobalt oxide at elevated temperature.[14] A block temperature of $>$380 K (Fig. 4C), as well as the divergence between ZFC and FC, reveals their large magnetic anisotropy barrier.[15]

The one-pot wet-chemistry synthesis of graphitically encapsulated cobalt nanocrystal assemblies is further rationalized here (Supporting Scheme 1†). It was demonstrated that cobalt precursors like cobalt oleate were not thermolyzed in 1-octadecene at $\sim$320 °C in the presence of oleic acid.[16] Correspondingly, cobalt oleate was thermolyzed in 1-octadecene at $\sim$320 °C in the absence of oleic acid, resulting in the formation of CoO.[13c,17] In our current work, cobalt oleate in excess oleic acid was heated to boiling at $\sim$360 °C. After this temperature was maintained for an hour, it started to increase steadily. On reaching $\sim$380 °C, black cobalt products were formed quickly

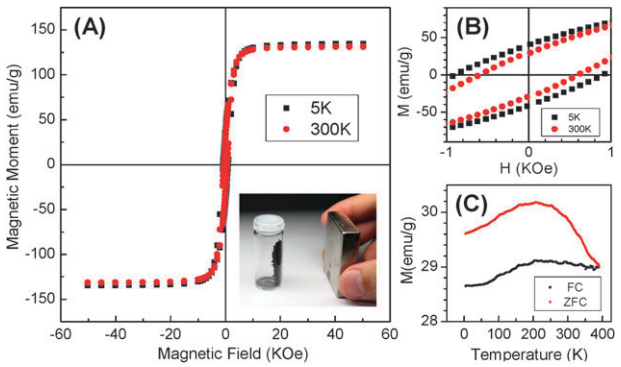

Fig. 4 (A) Original and (B) enlarged *M–H* curves of graphitically encapsulated cobalt nanocrystal assemblies under a magnetic field of up to 50 kOe at 5 and 300 K, respectively. (C) Temperature-dependent magnetization curves during zero-field cooling (ZFC) and field cooling (FC) processes at an external field of 100 Oe. Inset in (A) is an optical photograph of graphitically encapsulated cobalt nanocrystal assemblies under an external magnetic field.

accompanying a fast increase in temperature up to 395 °C. This can be understood as follows. In the presence of excess oleic acid, the thermolysis of cobalt(II) oleate at 360 °C, the reflux point of oleic acid, may form CoO, which is dissolved immediately by the free oleic acid (very similar to iron(II) oleate as reported by Peng[18c]). The newly formed cobalt oleate species can be further thermolyzed to form CoO again, followed by further dissolution by the remaining oleic acid. After the complete consumption of oleic acid, the resulting viscous solution temperature started to increase steadily up to ~380 °C. A fast increase in temperature up to 395 °C followed due to the formation of graphitically encapsulated cobalt nanostructures, and this temperature is close to the carbonization temperature (>400 °C) for organic molecules through pyrolysis (the resultant reducing gases lead to the transformation from CoO to Co nanocrystals).[18] This facile dehydrogenation/graphitization process can be explained by the stronger exothermic C–C formation (~607 kJ mol^{-1}) after the weaker endothermic C–H breaking (~338 kJ mol^{-1}), thus drastically releasing heat to increase temperature quickly. Meanwhile, the intrinsically catalytic role of as-formed small primary cobalt nanocrystals can slightly decrease the carbonization temperature to form graphitic shells on cobalt cores.[19] The graphitic shells around cobalt nanocrystals are very reactive so as to be quickly assembled into graphitically encapsulated cobalt nanocrystal aggregates.

In summary, graphitically encapsulated cobalt nanocrystal assemblies are directly prepared by one-pot reaction at a temperature of >380 °C. The fast formation of highly reactive graphitic shells on ferromagnetic cobalt nanocores of ~18 nm in size further mediates their magnetically oriented self-assembly into the bigger aggregates in liquid solutions, and thus their saturation magnetization is very close to the corresponding bulk one. A reversed etching process in strong acid produces a porous structure of graphitic networks (as potential porous electrodes), which clearly reveals the self-assembling nature of the aggregates. Meanwhile, the effective graphitization for the direct one-pot formation of graphitically encapsulated cobalt nanocrystal assemblies is rationalized, and the understanding further provides insight for preparing other graphitically encapsulated metal or inorganic nanostructures.

Notes and references

1 (*a*) S. H. Liu and M. Y. Han, *Chem.–Asian J.*, 2010, **5**, 36; (*b*) A. Guerrero-Martínez, J. Pérez-Juste and L. M. Liz-Marzán, *Adv. Mater.*, 2010, **22**, 1182.

2 (*a*) X. M. Sun and Y. D. Li, *Angew. Chem., Int. Ed.*, 2004, **43**, 597; (*b*) S. R. Guo, J. Y. Gong, P. Jiang, M. Wu, Y. Lu and S. H. Yu, *Adv. Funct. Mater.*, 2008, **18**, 872.

3 (*a*) W. S. Seo, J. H. Lee, X. M. Sun, Y. Suzuki, D. Mann, Z. Liu, M. Terashima, P. C. Yang, M. V. McConnell, D. G. Nishimura and H. J. Dai, *Nat. Mater.*, 2006, **5**, 971; (*b*) J. Zhang, X. Liu, R. Blume, A. H. Zhang, R. Schlögl and D. S. Su, *Science*, 2008, **322**, 73; (*c*) Y. H. Wang, W. Wei, D. Maspoch, J. S. Wu, V. P. Dravid and C. A. Mirkin, *Nano Lett.*, 2008, **8**, 3761; (*d*) R. L. Liu, D. Q. Wu, S. H. Liu, Q. Li, K. Koynov and W. Knoll, *Angew. Chem., Int. Ed.*, 2009, **48**, 4598.

4 (*a*) C. Desvaux, C. Amiens, P. Fejes, P. Renaud, M. Respaud, P Lecante, E. Snoeck and B. Chaudret, *Nat. Mater.*, 2005, **4**, 750; (*b*) A. H. Lu, W. C. Li, N. Matoussevitch, B. Spliethoff, H. Bonnemann and F. Schüth, *Chem. Commun.*, 2005, 98; (*c*) V. A. de la Peña O'Shea, P. R. de la Piscina, N. Homs, G. Arom and J. L. G. Fierro, *Chem. Mater.*, 2009, **21**, 5637.

5 J. F. Geng, D. A. Jefferson and B. F. G. Johnson, *Chem. Commun.*, 2004, 2442.

6 R. N. Grass, E. K. Athanassiou and W. J. Stark, *Angew. Chem., Int. Ed.*, 2007, **46**, 4909.

7 E. Y. Ye, B. H. Liu and W. Y. Fan, *Chem. Mater.*, 2007, **19**, 3845.

8 (*a*) T. Hayashi, S. Hirono, M. Tomita and S. Umemura, *Nature*, 1996, **381**, 772; (*b*) K. Chen, C. L. Wang, D. Ma, W. X. Huang and X. H. Bao, *Chem. Commun.*, 2008, 2765.

9 V. F. Puntes, K. M. Krishnan and A. P. Alivisatos, *Science*, 2001, **291**, 2115.

10 B. Ballesteros, G. Tobias, L. Shao, E. Pellicer, J. Nogues, E. Mendoza and M. L. H. Green, *Small*, 2008, **4**, 1501.

11 S. Han, Y. Yun, K.-W. Park, Y.-E. Sung and T. Hyeon, *Adv. Mater.*, 2003, **15**, 1922.

12 A. P. Alivisatos, *Nat. Biotechnol.*, 2004, **22**, 47.

13 (*a*) V. Skumryev, S. Stoyanov, Y. Zhang, G. Hadjipanayis, D. Givord and J. Nogués, *Nature*, 2003, **423**, 850; (*b*) J. Nogués, J. Sort, V. Langlais, V. Skumryev, S. Suriñach, J. S. Muñoz and M. D. Baró, *Phys. Rep.*, 2005, **422**, 65; (*c*) S. H. Liu, N. Ding, E. Y. Ye, Y. Zong, D. S. Wang, W. Knoll and M. Y. Han, *Chem. Commun.*, 2009, 6255.

14 Y. Yin, R. M. Rioux, C. K. Erdonmez, S. Hughes, G. A. Somorjai and A. P. Alivisatos, *Science*, 2004, **304**, 711.

15 F. Dumestre, B. Chaudret, C. Amiens, M. C. Fromen, M. J. Casanove, P. Renaud and P. Zurcher, *Angew. Chem., Int. Ed.*, 2002, **41**, 4286.

16 A. C. S. Samia, K. Hyzer, J. A. Schlueter, C. J. Qin, J. S. Jiang, S. D. Bader and X. M. Lin, *J. Am. Chem. Soc.*, 2005, **127**, 4126.

17 (*a*) K. An, N. Lee, J. Park, S. C. Kim, Y. Hwang, J. G. Park, J. Y. Kim, J. H. Park, M. J. Han, J. Yu and T. Hyeon, *J. Am. Chem. Soc.*, 2006, **128**, 9753; (*b*) Y. Zhang, J. Zhu, X. Song and X. H. Zhong, *J. Phys. Chem. C*, 2008, **112**, 5322.

18 (*a*) G. S. Chaubey, C. Barcena, N. Poudyal, C. B. Rong, J. M. Gao, S. H. Sun and J. P. Liu, *J. Am. Chem. Soc.*, 2007, **129**, 7214; (*b*) D. Kim, J. Park, K. An, N. K. Yang, J. G. Park and T. Hyeon, *J. Am. Chem. Soc.*, 2007, **129**, 5812; (*c*) F. Zhao, M. Rutherford, S. Y. Grisham and X. G. Peng, *J. Am. Chem. Soc.*, 2009, **131**, 5350.

19 W. Y. Zhou, X. D. Bai, E. G. Wang and S. S. Xie, *Adv. Mater.*, 2009, **21**, 4565.